

See discussions, stats, and author profiles for this publication at: <https://www.researchgate.net/publication/11460907>

# Selected-control hydrothermal synthesis of alpha- and beta-MnO(2) single crystal nanowires.

ARTICLE *in* JOURNAL OF THE AMERICAN CHEMICAL SOCIETY · APRIL 2002

Impact Factor: 12.11 · Source: PubMed

---

CITATIONS

98

---

READS

1,102

## 2 AUTHORS:



Xun Wang

Tsinghua University

158 PUBLICATIONS 11,108 CITATIONS

SEE PROFILE



Yadong Li

Tsinghua University

355 PUBLICATIONS 24,345 CITATIONS

SEE PROFILE

Selected-Control Hydrothermal Synthesis of  $\alpha$ - and  $\beta$ -MnO<sub>2</sub> Single Crystal Nanowires

Xun Wang and Yadong Li\*

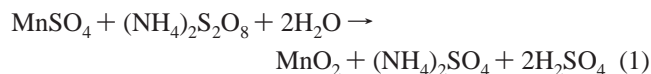
Department of Chemistry, Tsinghua University, Beijing 100084, People's Republic of China

Received December 7, 2001

The many polymorphic forms of manganese dioxide, such as  $\alpha$ -,  $\beta$ -,  $\gamma$ -, and  $\delta$ -type, have distinctive properties and now are widely used as catalysts, ion-sieves, and especially as electrode materials in Li/MnO<sub>2</sub> batteries.<sup>1–3</sup> As the operating properties of a Lithium battery depend not only on the manganese oxidation state but also on the MnO<sub>2</sub> structure type, great effort has been made to prepare bulky or nanocrystalline MnO<sub>2</sub> with different structures.<sup>1–6</sup> However, to the best of our knowledge, the synthesis of a one-dimensional (1D) single-crystal nanostructure of MnO<sub>2</sub> with different crystallographic structures has not been reported to date, which may provide the possibility of detecting the theoretical operating limits of a Lithium battery as the 1D systems are the smallest dimension structures for efficient transport of electrons,<sup>7,8</sup> and may give an ideal host material for the insertion and extraction of Lithium ions. Herein we report the synthesis of a MnO<sub>2</sub> 1D nanostructure:  $\alpha$ -MnO<sub>2</sub> with diameters of 5–20 nm and lengths ranging between 5 and 10  $\mu$ m, and  $\beta$ -MnO<sub>2</sub> with diameters of 40–100 nm and lengths ranging between 2.5 and 4.0  $\mu$ m.

The 1D nanostructure appears as an exciting research field for the great potential of addressing space-confined transport phenomena as well as applications.<sup>9</sup> The key to preparing a 1D nanostructure can be focused on the way in which atoms or other building blocks are rationally assembled into structure with nanometer size but much larger lengths.<sup>7</sup> Templates or catalysts have been widely used to grow 1D nanostructures, such as Ge, Si, and GaN nanowires,<sup>7,10–12</sup> in which templates are used to confine the growth of wires, while catalysts may act as the energetically favorable sites for the adsorption of reactant molecules.<sup>7,10–12</sup> However, the introduction of templates or catalysts to the reaction system means a much more complicated process involving the preparation of catalysts or the selection of templates, and may bring about an increase of impurity concentration in the final product. Meanwhile, recent studies, for example, the preparation of Bi, WS<sub>2</sub> nanotubes, W nanowires,<sup>13–15</sup> and semiconducting oxides nanobelts,<sup>16</sup> have shown that the 1D nanostructure might be prepared under properly controlled conditions, even without the presence of catalysts or templates, which might mean that the formation of the 1D nanostructure is thermodynamically preferable for many substances under certain conditions. Here, a selected-control low-temperature hydrothermal method has been developed in our synthesis of a MnO<sub>2</sub> 1D nanostructure through the oxidation of Mn<sup>2+</sup> by S<sub>2</sub>O<sub>8</sub><sup>2-</sup>, with no existence of catalysts or templates.

The chemical reaction can be formulated as



which comprises two half reactions

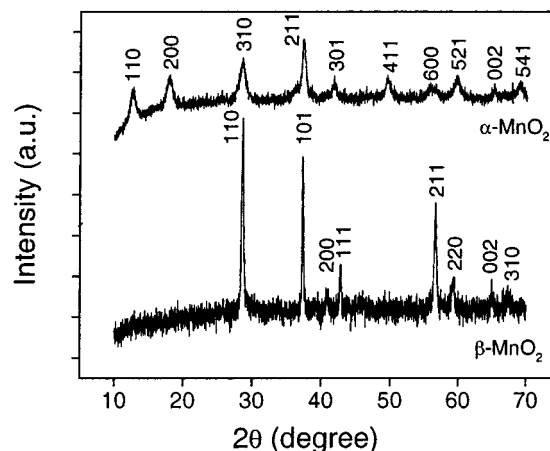
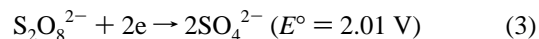
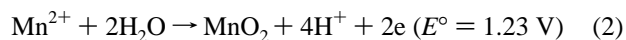


Figure 1. XRD patterns of  $\alpha$ -MnO<sub>2</sub> and  $\beta$ -MnO<sub>2</sub>.



On the basis of the values of  $E^\circ$ , the standard Gibbs free energy change  $\Delta G^\circ$  of reaction 1 could be estimated to be  $-151 \text{ kJ mol}^{-1}$ , implying a very strong tendency for reaction 1 to progress toward the right-hand side.

Analytical grade hydrate manganese sulfate ( $\text{MnSO}_4 \cdot \text{H}_2\text{O}$ , 0.008 mol) and an equal amount of ammonium persulfate ( $(\text{NH}_4)_2\text{S}_2\text{O}_8$ ) were put into distilled water at room temperature to form a homogeneous solution, which was then transferred into a Teflon-lined stainless steel autoclave, sealed, and maintained at 120 °C for 12 h. After the reaction was completed, the resulting black solid product was filtered, washed with distilled water to remove ions possibly remaining in the final products, and finally dried at 120 °C in air. The whole process, appropriate for the preparation of  $\beta$ -MnO<sub>2</sub> nanorods, can be conveniently adjusted to prepare  $\alpha$ -MnO<sub>2</sub> nanowires by simply adding analytical grade ammonium sulfate ( $(\text{NH}_4)_2\text{SO}_4$ , 0.015 mol) to the reaction system.

The phase purity of the products was examined by X-ray diffraction (XRD) with use of a Brucker D8-advance X-ray diffractometer with Cu K $\alpha$  radiation ( $\lambda = 1.5418 \text{ \AA}$ ), the operation voltage and current maintained at 40 kV and 40 mA, respectively. All of the reflections of the XRD pattern in Figure 1, top, can be readily indexed to a pure tetragonal phase [space group:  $I4/m$  (87)] of  $\alpha$ -MnO<sub>2</sub> with lattice constants  $a = 9.7847 \text{ \AA}$  and  $c = 2.8630 \text{ \AA}$  (JCPDS 44-0141), while those in Figure 1, bottom, can be indexed to a pure tetragonal phase [space group:  $P4_2/mnm$  (136)] of  $\beta$ -MnO<sub>2</sub> with lattice constants  $a = 4.3999 \text{ \AA}$  and  $c = 2.8740 \text{ \AA}$  (JCPDS 24-0735). The XRD pattern indicates that pure  $\alpha$ - and  $\beta$ -MnO<sub>2</sub> can be obtained, under current synthetic conditions.

\* Address correspondence to this author. E-mail: ydli@tsinghua.edu.cn.

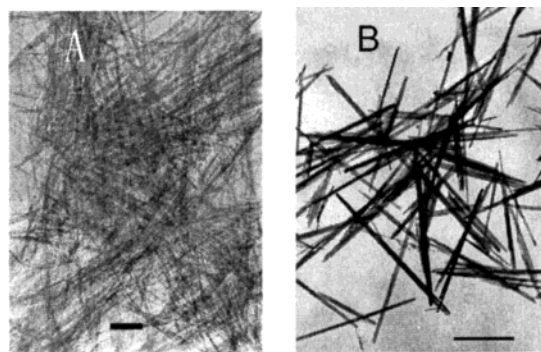


**Figure 2.** (A) TEM pattern of  $\alpha$ - $\text{MnO}_2$ , scale bar 20 nm; (B) TEM pattern of  $\beta$ - $\text{MnO}_2$ , scale bar 1  $\mu\text{m}$ .

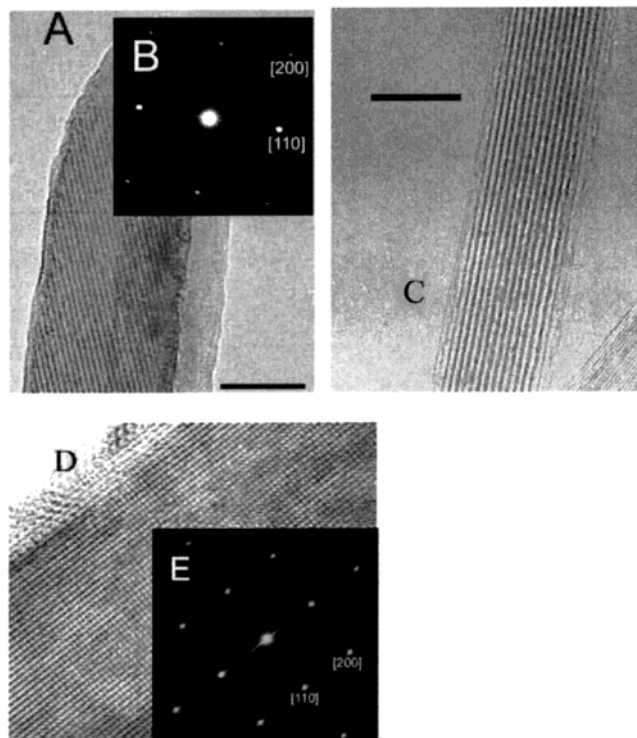


**Figure 3.** (A and B) single rod (scale bar 10 nm) and electron diffraction pattern of  $\alpha$ - $\text{MnO}_2$ ; (C) HRTEM images of  $\alpha$ - $\text{MnO}_2$  with growth direction [110], spacing  $d = 0.701$  nm, scale bar = 5 nm; (D) HRTEM images of  $\beta$ - $\text{MnO}_2$  with growth direction [110], spacing  $d = 0.318$  nm; and (E) electron diffraction pattern of  $\beta$ - $\text{MnO}_2$ .

The micro-/nanostructure of the products was further examined with transmission electron microscopy (TEM, Hitachi (Tokyo, Japan) H-800) and high-resolution transmission electron microscopy (HRTEM, JEOL-2010). As shown in Figure 2, all  $\alpha$ - $\text{MnO}_2$  samples dispersed on the TEM grids show nanowire morphology with diameters 5–20 nm and lengths ranging between 5 and 10  $\mu\text{m}$ , while  $\beta$ - $\text{MnO}_2$  samples show nanorod morphology with diameters 40–100 nm and lengths ranging between 2.5 and 4.0  $\mu\text{m}$ . Figure 3, B and E, taken from a single rod (Figure 3, A and D, respectively), can be indexed as the diffraction patterns of the 001 zone axis of tetragonal  $\alpha$ - $\text{MnO}_2$  and tetragonal  $\beta$ - $\text{MnO}_2$ . More details about single rods are revealed in Figure 3A,C,D.

$\alpha$ - and  $\beta$ - $\text{MnO}_2$  are different in that the  $\alpha$ -type is constructed from double chains of  $[\text{MnO}_6]$  octahedra forming  $2 \times 2$  tunnels

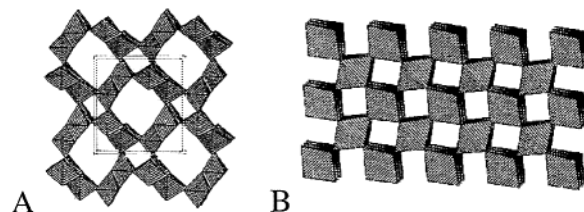


**Figure 4.** (A) The structure of  $\alpha$ - $\text{MnO}_2$  with double chains of  $[\text{MnO}_6]$  octahedra; (B) the structure of  $\beta$ - $\text{MnO}_2$  with single chains of  $[\text{MnO}_6]$  octahedra.

(Figure 4A), while the  $\beta$ -type is composed of single chains of the octahedral (Figure 4B).<sup>1</sup> It is apparent that  $\text{NH}_4^+$  and  $\text{SO}_4^{2-}$ , coexisting with the corresponding ions  $\text{Mn}^{2+}$  and  $\text{S}_2\text{O}_8^{2-}$  in both reaction systems, play an important role in our synthesis in determining the crystal structure and morphology of the products. A certain amount of  $\text{NH}_4^+$  is required as stabilizing ions for the  $2 \times 2$  tunnels in the formation of  $\alpha$ -type while the  $\text{SO}_4^{2-}$  is involved in eq 1, from which it can be seen that the increase of  $\text{SO}_4^{2-}$  will result in a decrease in the formation rate of  $\text{Mn}^{4+}$  or the growth unit  $[\text{MnO}_6]$ , and thus a decrease in the formation rate of various crystal faces. In our experiment, the increase of  $\text{SO}_4^{2-}$  leads to a product with a much slimmer outlook, which may mean that the decrease occurs at different speeds for different faces with the elongated direction influenced less weakly. Since the whole process only involves the process of crystal growth, it might be generally believed that reactant concentration has different effects on the formation rate of different crystal faces, which might be applied to the preparation of the 1D single-crystal nanostructure. By means of proper control of the reactant concentration and temperature, we have successfully prepared the 1D nanostructure of some other oxides such as ZnO,  $\text{TiO}_2$ ,  $\text{MoO}_3$  nanowires, nanotubes and, nanobelts.<sup>17</sup>

This low-temperature synthetic route, based on simple reactions with no participation of catalysts or templates and requiring no expensive and precise equipment, will ensure higher purity in the products and greatly reduce the production cost, and thus offer great opportunity for scale-up preparation of 1D nanostructure materials.

**Acknowledgment.** This work was supported by NSFC (20025102, 50028201, 20151001) and the State key project of fundamental research for nanomaterials and nanostructures.

## References

- (1) Thackeray, M. M. *Prog. Solid State Chem.* **1997**, 25, 1.
- (2) Armstrong, A. R.; Bruce, P. G. *Nature* **1996**, 381, 499.
- (3) Ammundsen, B.; Paulsen, J. *Adv. Mater.* **2001**, 13, 943.
- (4) Chitrahah, R.; Kanoh, H.; Kim, Y.; Miyai, Y.; Ooi, K. J. *Solid State Chem.* **2001**, 160, 69.
- (5) Hunter J. C. *J. Solid State Chem.* **1981**, 39, 142.
- (6) Bach, S.; Pereira-Ramos, J. P.; Baffier, N. *J. Solid State Chem.* **1995**, 120, 70.
- (7) Lieber, C. M. et al. *Acc. Chem. Res.* **1999**, 32, 435.
- (8) Huang, M. H.; Mao, S.; Feick, H.; Yan, H. Q.; Wu, Y. Y.; Kind, H.; Weber, E.; Russo, R.; Yang, P. D. *Science* **2001**, 292, 1897.
- (9) Dekker, C. *Phys. Today* **1999**, 52, 22.
- (10) Han, W. Q.; Fan, S. S.; Li, Q. Q.; Hu, Y. D. *Science* **1997**, 277, 1287.
- (11) Morales, A. M.; Lieber, C. M. *Science* **1998**, 279, 208.
- (12) Duan, X. F.; Huang, Y.; Cui, Y.; Wang J. F.; Lieber, C. M. *Nature* **2001**, 409, 66.
- (13) Li, Y. D. et al. *J. Am. Chem. Soc.* **2001**, 123, 9904.
- (14) Li, Y. D. et al. *J. Am. Chem. Soc.* **2002**, 124, 1411.
- (15) Li, Y. D. et al. *Angew. Chem., Int. Ed.* **2002**, 41, 333.
- (16) Pan, Z. W.; Dai, Z. R.; Wang, Z. L. *Science* **2001**, 291, 1947.
- (17) Li, Y. D. Unpublished results.

JA0177105